Colloids and Surfaces A: Physicochem. Eng. Aspects 365 (2010) 145–153

Contents lists available at ScienceDirect

Colloids and Surfaces A: Physicochemical and Engineering Aspects

journal homepage: www.elsevier.com/locate/colsurfa

Interface and bulk exchange: Single drops experiments and CFD simulations

A. Javadi[a], J.K. Ferri[b], Th.D. Karapantsios[c], R. Miller[a,*]

[a] Max Planck Institute of Colloids and Interfaces, Am Muehenberg 1, 14424 Potsdam,Germany
[b] Lafayette College, Easton, PA 18042, USA
[c] Aristotle University of Thessaloniki, GR-54124 Thessaloniki, Greece

ARTICLE INFO

Article history:
Received 9 February 2010
Received in revised form 20 April 2010
Accepted 26 April 2010
Available online 26 May 2010

Keywords:
Interface and bulk exchange
Pulse-like flow
CFD simulations
Drop profile analysis
Visualized flow pattern in a drop

ABSTRACT

The coaxial double capillary for controlling pendant drops is an interesting experimental technique for investigating adsorption kinetics and transport properties of soluble components in the bulk which can exchange with the interface. The key process of this technique is the exchange of the entire bulk of a droplet without any direct perturbations of the interface due to forced convection. Therefore efficient exchange conditions should be determined in order to provide results during the exchange protocol that can be used for a reliable data interpretation of the adsorption process. In this paper we report on the flow into a drop formed with a double capillary set-up, as visualized by using a dye and simulated by computational fluid dynamics (CFD) of the flow field and mass transfer during the drop bulk exchange. Regarding the experimental protocols, for better monitoring and control of the droplet size a pulse-like flow with different injection volumes (dV) and pulse intervals (dt) combined with drop profile analysis tensiometry (PAT1) was used. The visualized experimental concentration fields are confirmed by the concentration contours obtained from CFD simulations. Both approaches give access to estimate the moment when the dye arrives at the drop surface. The drop surface exchange is also monitored via the measured surface tension. The computational results for average drop interface concentration (DIC) and drop outlet concentration (DOC) are discussed for different conditions.

1. Introduction

Investigations of the equilibrium and dynamics of adsorption layers of surfactants and macromolecules at fluid interfaces are in the focus of interest due to their importance in fundamental and applied science. Single liquid drops can be used as a great experimental lab for this purpose by using techniques such as drop profile analysis tensiometry (PAT) which is developed during the last 25 years from a new idea [1] to one of the most versatile tools applied to various investigations in surface science [2,3]. Wege et al. showed that the drop profile tensiometry has additional potential when a special drop exchange mechanism is used [4]. It consists in a special design of a double capillary combined with a double dosing system where the liquid in the drop formed at its tip can be exchanged by the inflow and outflow through one of the two coaxially arranged capillaries, respectively. This procedure is complementary to the methodology of Svitova et al. [5] who used a convection cell for the exchange of the external liquid in a cuvette around a drop or bubble. Both techniques combined, even allow the exchange of the liquid inside a drop and additionally in the cuvette surrounding it, which gives a large number of experimental possibilities. This technique has been used frequently for different purposes such as studying competitive adsorption of surfactants/proteins at an interface [6,7] and layer-by-layer microencapsulation processes [8]. The drop exchange method is also advantageous for long time studies, as it allows to compensate for evaporation effects by adding only the solvent for the lost volume instead of the solution [9]. There are many more successful applications as recently summarized [10].

Drop interface and bulk exchange in this paper means: initially we form a fresh drop through the outer capillary using the syringe pump 1 filled with the solution of concentration $C_{1,\infty}$, which in our case is pure water, i.e. $C_{1,\infty} = 0$. For surfactant or protein solutions, we wait a respective time for reaching the adsorption equilibrium. Now, the second solution of concentration $C_{2,\infty}$ is injected into the drop through the inner capillary using the second syringe pump 2. During this procedure, the syringe pump 1 success liquid via the outer capillary to keep the drop at constant size. The target of this process is the complete exchange of the liquid inside the drop without significant perturbations of the interfacial layer. This means that the exchange between interface and bulk is not formed by convection but happens via transport by diffusion and adsorption or desorption, respectively. A low flow injection/suction process through the inner/outer capillary tips, respectively, is suitable for this aim. However at low flow rates, a long exchange time is required which depends on the solution's concentrations and the density difference between the initial drop liquid and the injected

* Corresponding author.
E-mail address: miller@mpikg.mpg.de (R. Miller).

0927-7757/$ – see front matter © 2010 Elsevier B.V. All rights reserved.
doi:10.1016/j.colsurfa.2010.04.035

liquid. On the other hand at too high flow rates perturbations of the interface could be induced which may lead to interfacial instabilities, and hence to large data scattering for the real-time surface tension measurement. Such perturbations also affect the regular adsorption process. Therefore, the most efficient exchange conditions should be determined in order to provide results during the exchange process that can be used for a reliable data interpretation of the adsorption dynamics.

In [7] a simplified model was presented for the estimation of the liquid exchange process inside a drop, assuming a perfect mixing of the injected liquid through the inner capillary and volume compensation through the outer capillary. It was shown by using solvent mixtures that this simplification is an overestimation of the real bulk exchange. Obviously, the efficiency of the mixing depends on the flow pattern inside the drop induced by the injected liquid. It is the target of the present work to propose a simple protocol for the visualization of the liquid inflow and to present some hydrodynamic simulations to describe the experimentally observed patterns. For this purpose the fluid flow through a double capillary set-up into a pendant drop is visualized by using a dye, and computational fluid dynamics (CFD) simulations of the flow field and mass transfer during the drop bulk exchange are presented. In addition, the drop surface exchange is monitored via the measured surface tension. The computational results of the averaged drop interfacial concentration (DIC) and the drop outlet concentration (DOC) are discussed for different conditions. The DIC corresponds therefore to the subsurface concentration close to the drop surface, which is in a local equilibrium with the surface layer and hence correlates to the measured surface tension, while DOC corresponds to the mean concentration of the liquid leaving the drop through the outer capillary.

2. Experimental method

In the classical pendant drop experiments, a drop of a pure liquid or surfactant solution is formed at the tip of a capillary with a volume $5\,\mu l < V_D < 30\,\mu l$. The profile of the drop is cast onto a CCD camera and digitized. The digital images of the drop are recorded over time and the Young–Laplace equation is fitted to the experimental images to determine the surface tension accurately (±0.1 mN/m). A special constructed double capillary similar to that proposed by Wege et al. [11] was used for the bulk exchange experiments.

An experiment is performed as follows. A liquid drop of species concentration $C_{1,\infty}$ is formed using syringe 1 and allowed to quiescence. The drop bulk is then exchanged by the injection of the second liquid of species concentration $C_{2,\infty}$ via syringe 2. Regarding the experimental protocols, for better monitoring and control of droplet size, a pulse-like flow with different injection velocity dV and waiting time dt between two pulses are applied via syringe 2 into the drop in the PAT1 set-up. Then drop volume V_D or area A_D is maintained constant via feedback control using the PAT1 software and the withdrawal of liquid from the droplet interior at the same volumetric flow rate (R_E) using syringe 1. During the exchange, the concentration of species in the drop, i.e. $C_1(t)$ and $C_2(t)$, evolve continuously from the initial distribution, $C_1(t=0) = C_{1,\infty}$ and $C_2(t=0) = 0$, to the final distribution, $C_1(t=\infty) = 0$ and $C_2(t=\infty) = C_{2,\infty}$. The surface tension before, during, and after the exchange is monitored using PAT1 set-up.

3. Governing equations

The simplest description of the evolution of the bulk concentration can be derived if the drop bulk is assumed to be perfectly mixed. For a perfectly mixed drop bulk, the concentration of species 1 is described by [7]:

$$C_1(t) = C_{\infty,1}\exp(-t/\tau) \tag{1}$$

where τ is the residence time of the liquid in the drop $\tau = V_D/R_E$, and the concentration of species $C_{2,\infty}$ (i.e. $C_{1,\infty} = 0$)

$$C_2(t) = C_{\infty,2}\,(1 - \exp(-t/\tau) \tag{2}$$

Experiments which measure the exchange rate can be performed using simple liquids, for example, using water and binary mixtures of water and ethanol or DMSO and chlorobenzene, and monitoring surface tension during the exchange.

The details of the dynamics of the bulk exchange are important to equilibrium and kinetic experiments. For equilibrium it is important to quantify the volume of fluid to be injected in order to achieve complete exchange. Additionally, in order to separate interfacial exchange kinetics from the dynamics of the bulk exchange process, the evolution of the bulk concentration must be described as a function of the extrinsic conditions such as fluid transport properties, capillary tip geometry, average and local fluid velocity, and bulk concentration.

The results of perfect mixing assumption described by Eqs. (1) and (2) are a rough estimation and in general show significant differences with practical data. In the absence of a proper exact solution, computational fluid dynamics (CFD) simulations of the fluid flow and mass transfer in the drop are a good alternative. CFD can provide interesting details on a microscopic level about the flow structure, velocity and concentration distribution, and on a macroscopic level, can be used to determine the overall residence time of liquid in the drop and average drop surface concentration. The spatiotemporal species distribution can also be calculated to determine the rate at which the drop bulk attains compositional uniformity. For this purpose direct numerical solution of the Navier–Stokes equation for an unsteady 2D axisymmetric geometry with the following axial and radial momentum conservation equations is performed:

$$\begin{aligned}&\frac{\partial}{\partial t}(\rho u_x) + \frac{1}{r}\frac{\partial}{\partial x}(r\rho u_x u_x) + \frac{1}{r}\frac{\partial}{\partial r}(r\rho u_r u_x)\\ &= -\frac{\partial p}{\partial x} + \frac{1}{r}\frac{\partial}{\partial x}\left[r\mu\left(2\frac{\partial u_x}{\partial x} - \frac{2}{3}(\nabla.\vec{u})\right)\right]\\ &\quad + \frac{1}{r}\frac{\partial}{\partial r}\left[r\mu\left(\frac{\partial u_x}{\partial r} + \frac{\partial u_r}{\partial x}\right)\right] + F_x\end{aligned} \tag{3-a}$$

$$\begin{aligned}&\frac{\partial}{\partial t}(\rho u_r) + \frac{1}{r}\frac{\partial}{\partial x}(r\rho u_x u_r) + \frac{1}{r}\frac{\partial}{\partial r}(r\rho u_r u_r)\\ &= -\frac{\partial p}{\partial r} + \frac{1}{r}\frac{\partial}{\partial r}\left[r\mu\left(2\frac{\partial u_r}{\partial r} - \frac{2}{3}(\nabla.\vec{u})\right)\right]\\ &\quad + \frac{1}{r}\frac{\partial}{\partial x}\left[r\mu\left(\frac{\partial u_r}{\partial x} + \frac{\partial u_x}{\partial r}\right)\right] - 2\mu\frac{u_r}{r^2} + \frac{2}{3}\frac{\mu}{r}\left(\nabla.\vec{u}\right) + F_r\end{aligned} \tag{3-b}$$

where $\nabla\vec{u} = \partial u_x/\partial x + \partial u_r/\partial r + u_r/r$ and $\vec{F} = \rho\vec{g}$ is the body force in axial direction x. These equations describe the velocity vector field $v(t,x,r)$ in terms of the intrinsic fluid properties, viscosity μ and density ρ, and the pressure P. Along with the provided information about the flow field the species continuity equation accounts for both convective and diffusive transport in the drop bulk by:

$$\frac{\partial C_i}{\partial t} + \vec{u}\nabla C_i = D_i\nabla^2 C_i \tag{4}$$

where D_i are the diffusion coefficients of the species in the liquid phase.

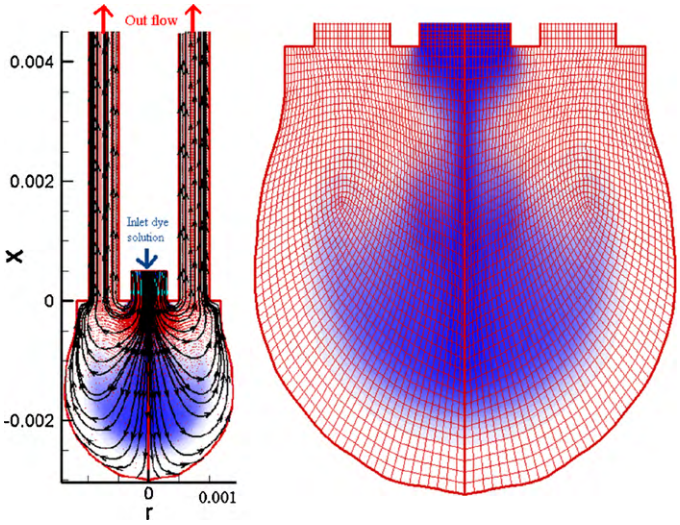

Fig. 1. Geometry and computational domain of the applied coaxial double capillary pedant drop similar to the experimental conditions.

4. Computational approach and boundary conditions

The given set of axisymmetric conservation equations were solved computationally using the FLUENT 6.2 CFD software via a finite volume approach with a segregated implicit solver. Fig. 1 shows the geometry and computational domain for the applied coaxial double capillary with pedant drop, equivalent to our experimental conditions. The inlet flow is a pulse-like flow with different pulse periods (dt = 0. 33 s and 0.2 s as time between two subsequent pulses) and different injected volumes per pulse (dV = 0.033, 0.067, 0.1, 0.2 mm^3/pulse). The pulse duration for the given injected volume can be calculated from the syringe dosing rate kept constant at 20 mm^3/s in all experiments.

No slip boundary conditions on the tube walls ($U_x = U_{y=0}$) and zero shear stress at the drop surface (referring to a free gas–liquid interface) are applied. At $t = 0$ the system contains pure water ($C_{2,0} = 0$) inside the drop and tube. To visualize the spatiotemporal distribution of bulk concentration, experiments were performed using an inlet aqueous solution of a low molecular weight dye (Brilliant Green, $C_{2,\infty} = 3.3$ mg/ml, $D_2 \approx 5 \times 10^{-6}$ cm^2/s).

5. Results and discussion

In this section first the comparison of experimental images of dye exchange with CFD simulation of concentration contours are discussed. These results present an overall idea of the drop exchange process and also illustrate the validity of the applied CFD simulation. Then measured surface tension data are discussed which support the visual observation including possible Marangoni convections. In the last section the CFD results of the area weighted average of the drop interfacial (subsurface) concentration (DIC) and drop outlet concentration (DOC) are discussed for different conditions.

5.1. Drop exchange visualization

Figs. 2–7 show the comparison of experimental drop images with visualized dye distribution and the corresponding CFD simulation with concentration contours during drop exchange at different flow rates. The results in Fig. 2 obtained for dt = 0.33 s and dV = 0.033 mm^3/pulse show a slightly asymmetric dye distribution. This can be due to the weak convective flow and the low density difference which both allow the appearance of a disordered flow caused by a minor asymmetry of the inner capillary position and small drop shaking during liquid injection. However, as the injected dye solution has a density slightly higher than water (the dye solution of 0.3 mg/ml has a density about 1% larger than water), it flows toward the drop bottom. The simulation results with a full symmetric assumption obviously illustrate a completely symmetric dye distribution which is in a quite good agreement with the experimental pictures, in particular, the moment when the dye solution reaches the drop apex. When the dye solution reaches the drop surface a Marangoni convection can set in due to a significant surface concentration gradient. Note, the presented CFD simulations are valid only until the onset of Marangoni flow, as this surface effect has not been included into the simulations. This matter will be discussed qualitatively further below and will have to be handled in a future more sophisticated CFD simulation.

The exchange process using a pulse period of dt = 0.33 s and higher volume injection of dV = 0.1 mm^3/pulse is shown in Fig. 3. Because of the stronger convective flow, a more symmetric dye distribution is observed. For a further decreased pulse period of dt = 0.2 s at the same volume injection dV = 0.1 mm^3/pulse the

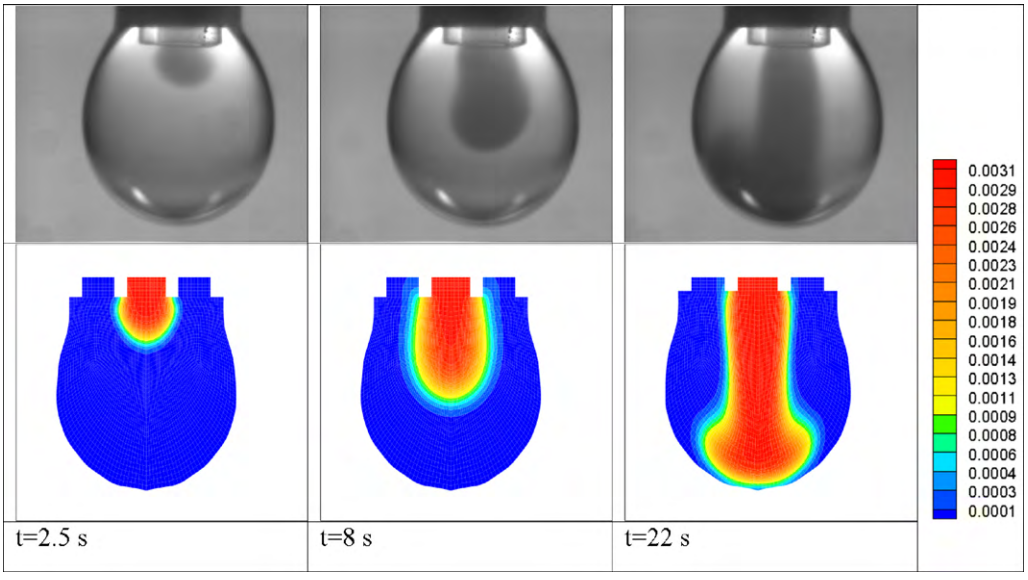

Fig. 2. Comparison of dye exchange experimental snapshots (top) and CFD simulation of dye concentration contours (bottom) for dt = 0.33 s, dV = 0.033 mm^3/pulse.

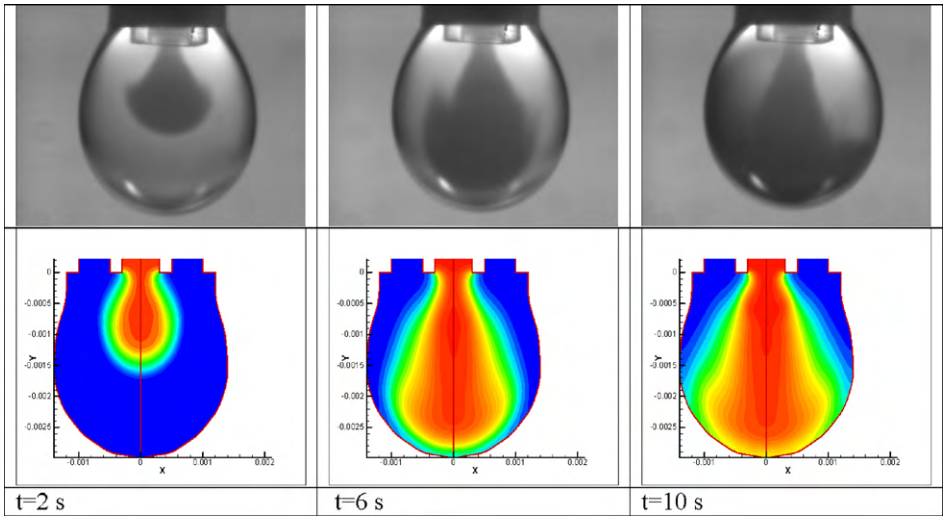

Fig. 3. Comparison of dye exchange experimental snapshots (top) and CFD simulation of dye concentration contours (bottom) for dt = 0.33 s, dV = 0.1 mm^3/pulse.

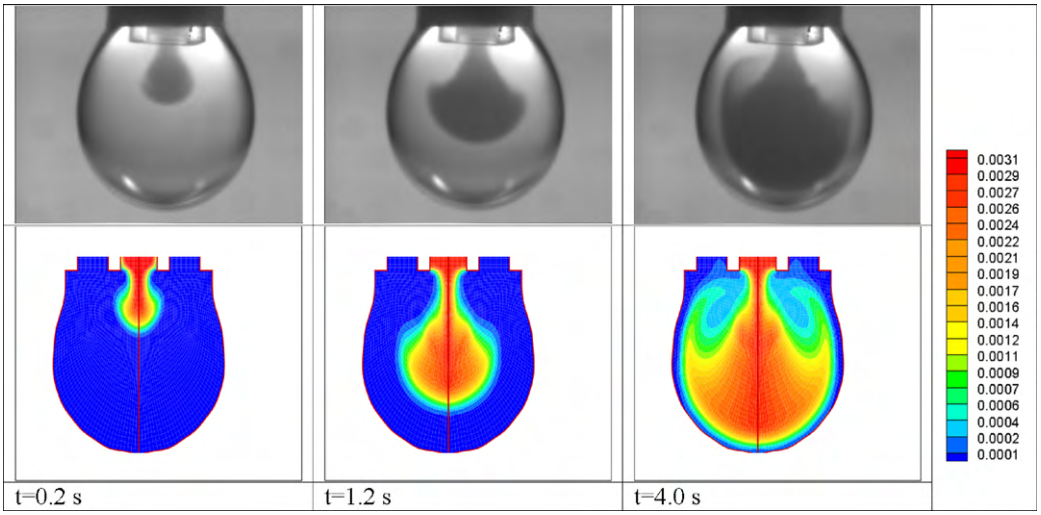

Fig. 4. Comparison of dye exchange experimental snapshots (top) and CFD simulation of dye concentration contours (bottom) for dt = 0.2 s, dV = 0.1 mm^3/pulse.

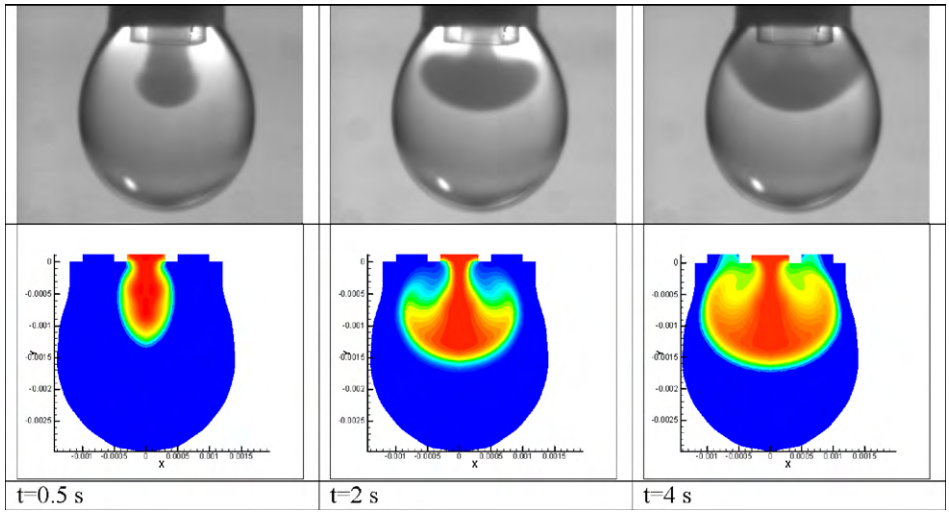

Fig. 5. Comparison of dye exchange experimental snapshots (top) and CFD simulation of dye concentration contours (bottom) for dye solution 0.3 mg/ml + 1.5% ethanol (density slightly lower than water), for dt = 0.2 s, dV = 0.1 mm^3/pulse.

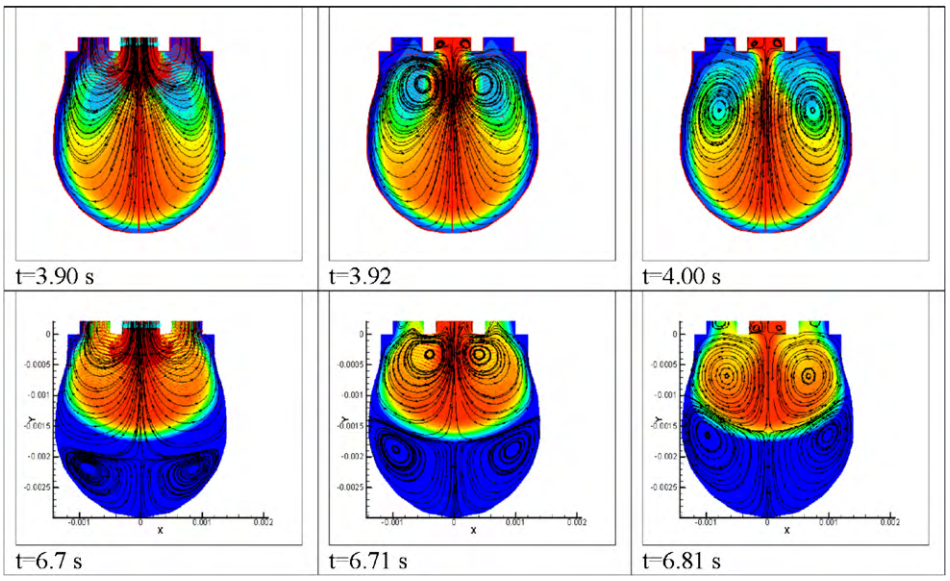

Fig. 6. The effects of density difference on the concentration contours and flow filed, appearing secondary circulating flow in the bottom of droplet for low density solution; 0.3 mg/ml dye (top line—density slightly higher than water), and 0.3 mg/ml dye + 1.5 vol% ethanol (bottom line—density slightly less than water); dt = 0.2 s, dV = 0.1 mm^3/pulse.

convection effects become stronger and the flow reaching the bottom of the drop shows a clear circulating flow due to the stagnant point in the impinging liquid flow. In Fig. 4 a good agreement between experimental images and the CFD simulation is observed.

5.2. Density difference effects

For many applications the inlet flow for liquid exchange in the droplet contains a mixture of components and solvents which can change the density of the injected solution. For this purpose 1.5 wt% ethanol was added to the dye solution so that the density of this solution was slightly less than water. The results presented in Fig. 5 for dt = 0.2 s and dV = 0.1 mm^3/pulse illustrate a quick reverse flow of the injected liquid with exchanging the liquid in even less than half of the droplet. A continuation of this liquid exchange over long times cannot provide a complete bulk exchange. This matter is discussed further below in some more detail. For a better understanding of the density effects on the drop exchange mechanism, a comparison of the streamlines and flow pattern is shown in Fig. 6 for a dye solution of 0.3 mg/ml in absence (density slightly higher than water), and presence of 1.5 wt% ethanol (density slightly lower than water). There is a secondary circulating flow at the bottom of the droplet which separates the entrance circulation of the dye solution at the top from the region at the drop bottom when a liquid of lower density is injected.

To improve the exchange process for injections of low density solutions, we have to increase the injection velocity. Fig. 7 shows the results for a drop exchange at dt = 0.2 s and dV = 0.2 mm^3/pulse. Because of the high inertial force, the injected dye solution reaches the bottom of the drop quicker. Simultaneously, a reverse flow out of the drop is visible, leading to a mushroom like shape of the concentration contour. The results of CFD simulations reproduce this pattern well. A good drop exchange is observed after 8 s, however because of the stagnation point and the reverse flow from the bottom, the drop surface concentration DIC needs much longer time to approach an equilibrium situation, as discussed further below.

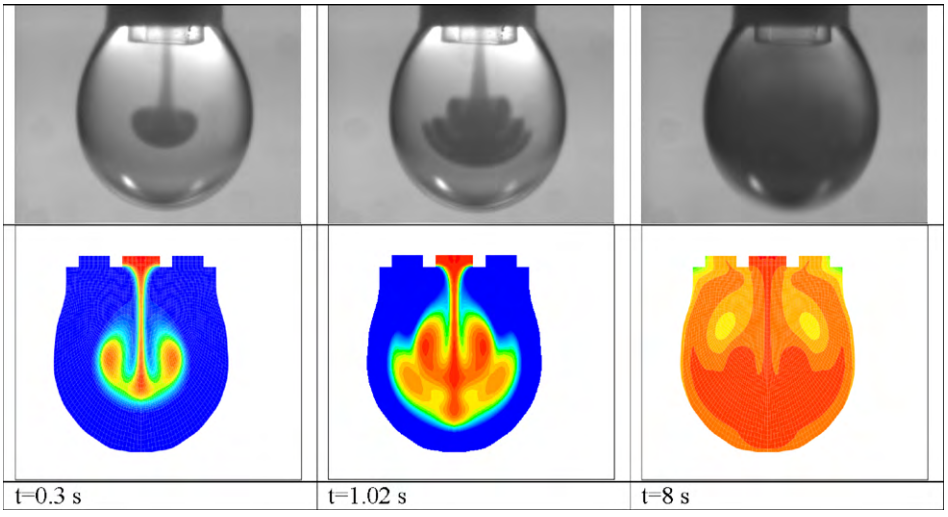

Fig. 7. Comparison of dye exchange experimental snapshots (top) and CFD simulation of dye concentration contours (bottom) for dye solution 0.3 mg/ml + 1.5 vol% ethanol (density slightly lower than water), for dt = 0.2 s, dV = 0.2 mm^3/pulse.

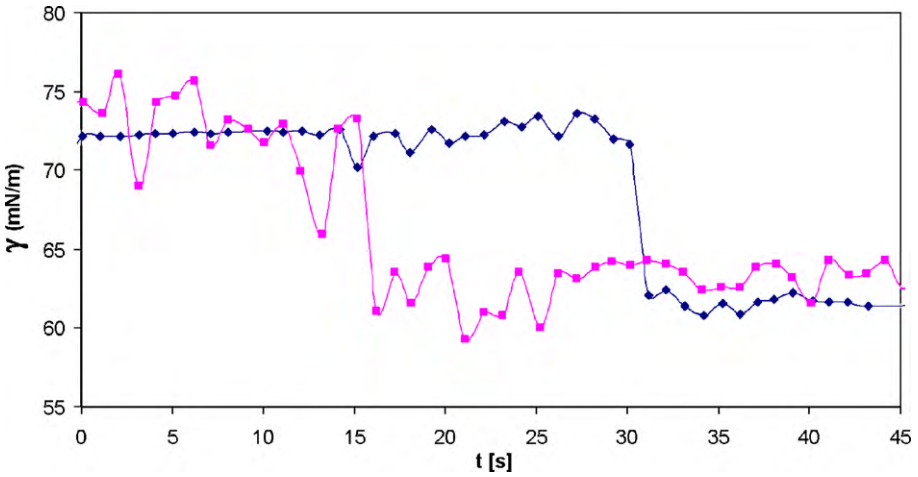

Fig. 8. Increasing data scattering during surface tension measurement due to drop shaking and instability for high volume rate injection, dt = 0.33 s, dV = 0.033 mm^3/pulse (♦), 0.1 mm^3/pulse (■)

5.3. Immersed depth of the inner capillary tip

As was mentioned above a high inertial force can lead to a significant shaking of the drop and consequently to interfacial instabilities which then can disturb the regular adsorption/desorption processes at the interface. Also for high flow injection rates a less accurate drop size control can cause a much higher scattering of the measured surface tensions (Fig. 8).

Therefore to improve exchange process an alternative should be considered for the case of lower density liquid injection. This alternative consists in a larger immersed depth of the inner capillary into the drop (Fig. 9), leading to a significant improvement of the drop exchange. However, an immersion of the inner capillary lower than the drop center can cause again drop instabilities because of the stronger impinging liquid flow onto the droplet apex. The optimum immersion depth depends obviously on the operational conditions and fluid properties and requires more systematic studies.

5.4. Surface tension data and Marangoni convection

Typical results of surface tension measurements during drop exchange are shown in Figs. 10 and 11. As it is expected, when the impinging flow of the dye solution reaches the drop surface (macroscopically), with a short delay required for diffusing from the boundary layer to the drop surface (microscopically), a Marangoni convection sets in and creates a fast mixing of the dye solution inside the droplet and at its surface. This moment can be captured experimentally via a sudden decrease in surface tension. In the present CFD simulations, as mentioned above, no surface specific effects are considered. Hence, the onset of Marangoni flow cannot be simulated with the present approach and can be compared with experimental data only until the moment when Marangoni effects appear.

Although via Marangoni convection the dye can be distributed along the interface and consequently also inside the droplet quickly, for conditions of incomplete exchange of the drop bulk, a desorption of surfactant from the drop surface back to the bulk via diffusion can subsequently occur (Fig. 11). Later, a Marangoni convection can occur again, leading maybe to oscillation phenomena as observed in other experiments [12]. Although such processes can support the efficiency of the bulk exchange, for a quantitative adsorption kinetics experiment these phenomena can be disturbing. Therefore a proper drop exchange process should be optimized basically such that any remarkable Marangoni convection as an additional mixing tool is avoided. Under such conditions also an easier computational procedure becomes possible, while the results can be considered as a guideline for conditions with existing interfacial instabilities. Simulations with the consideration of Marangoni phenomena are under way and will be discussed in future work.

5.5. Drop interface and outlet concentrations

In this section the CFD simulation is applied for determining the averaged drop interfacial (DIC) and drop outlet concentrations (DOC). Fig. 12 shows DIC and DOC as functions of time for different dV and a constant dye concentration of 3 mg/ml. Almost all curves show three stages:

1. At the beginning of the drop exchange process, a zero dye concentration is observed for DIC and DOC, which indicates that a respective induction time is necessary for the dye solution to reach the drop interface and outlet.

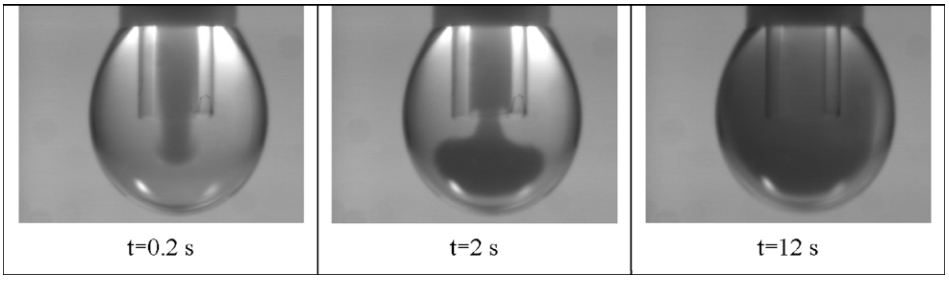

Fig. 9. Improved drop exchange process via a larger immersion depth of the inner capillary into the drop, dt = 0.2 s, dV = 0.1 mm^3/pulse.

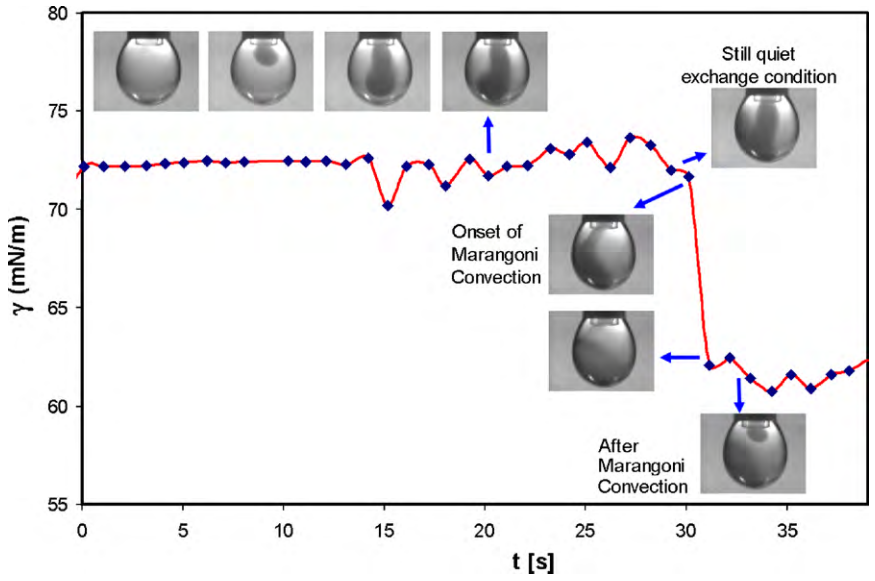

Fig. 10. Capturing the moment of Marangoni convection via measured surface tension during drop bulk exchange with a dye solution of 3 mg/ml; dt = 0.33 s, dV = 0.033 mm^3/pulse.

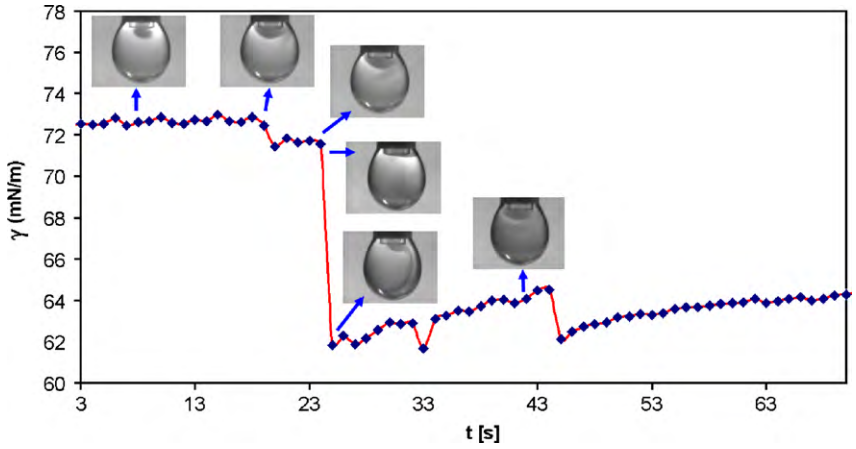

Fig. 11. Desorption process observed after an enhanced interfacial exchange caused by Marangoni convection at about 22 s (and maybe again at about 44 s), observed for the injection of a low density solution of 3 mg/ml dye + 1.5 wt% ethanol; experimental exchange conditions were dt = 0.33 s and dV = 0.033 mm^3/pulse.

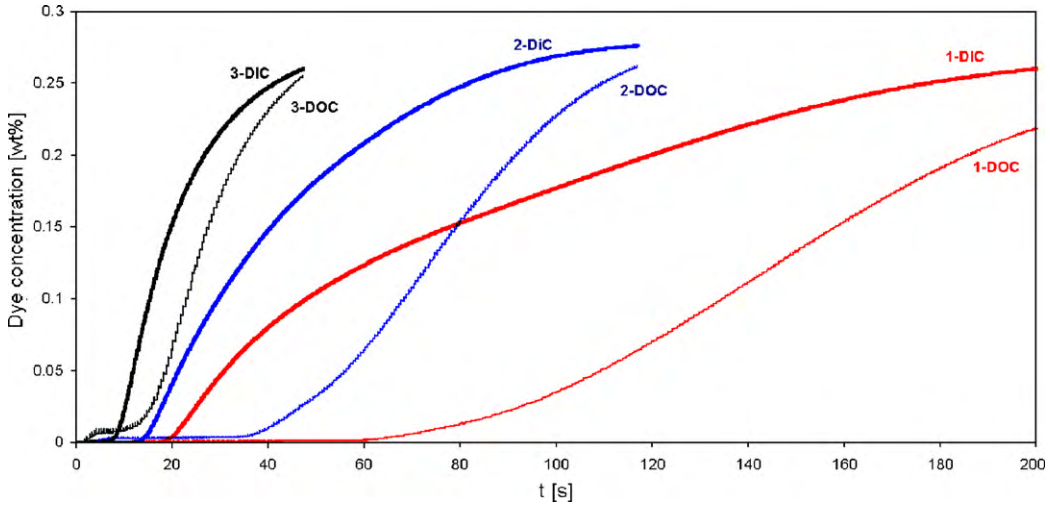

Fig. 12. DIC and DOC as functions of time for different dV and a dye concentration of 3 mg/ml; dt = 0.33 s, dV = 0.033 mm^3/pulse (1), 0.067 mm^3/pulse (2) and 0.1 mm^3/pulse (3), DIC—solid lines, DOC—dotted lines.

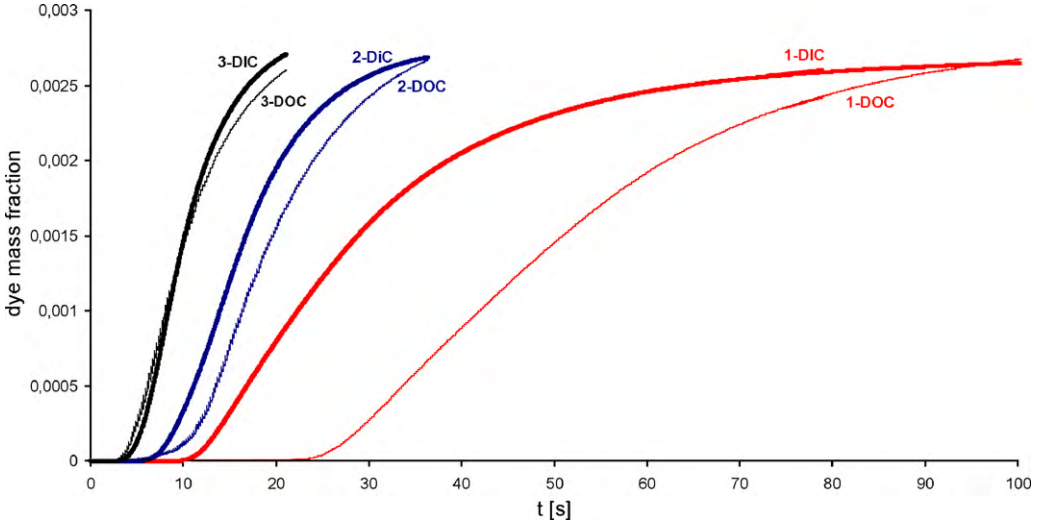

Fig. 13. DIC and DOC as functions of time for different dV and a dye concentration of 3 mg/ml; dt = 0.2 s, dV = 0.033 mm^3/pulse (1), 0.067 mm^3/pulse (2) and 0.1 mm^3/pulse (3), DIC—thick lines, DOC—thin lines.

2. After the initial time period, sharp increases in DIC and DOC are observed. The beginning of this region in the DIC curves corresponds to the onset of Marangoni convection;
3. The third stage is a longer time process especially at low values of dV, approaching the maximum accessible dye concentration of 100% (0.3 wt%). A large distance between the DIC and DOC curves indicates a significant difference in the exchange time for the drop surface and in the drop bulk. For establishing a complete drop exchange, these two curves should approach each other as close as possible. Therefore, dV = 0.1 mm^3/pulse provides a better drop exchange at shorter times. However, with respect to drop shaking and instability problems, and consequently larger scattering of measured surface tension data, this exchange rate might be already too high for optimum exchange conditions (see also comments to Fig. 8). Stopping the exchange process at high DIC while DOC values are still low (e.g. at t = 60 s for dV = 0.067 mm^3/pulse in Fig. 12) can lead to a desorption from the interfacial layer into the bulk.

The results for dt = 0.2 s and different dV are presented in Fig. 13. A faster drop exchange is observed for dt = 0.33 s as expected. Comparing the results for dV = 0.033 mm^3/pulse at dt = 0.2 s and dV = 0.067 mm^3/pulse at dt = 0.33 s, we can see that the total injected volumes per second are almost the same, however a more efficient drop exchange is obtained under the first condition. In general the shorter pulse period dt = 0.2 s, provides a closer distance between the DIC and DOC curves which indicates a more homogenous exchange process.

For the low density dye solution (+1.5 wt% ethanol), the DOC curve is higher than the DIC as discussed above. Fig. 14 shows typical results for dt = 0.2 s and dV = 0.1 mm^3/pulse which are in agreement with the corresponding time for the dye to reach the drop surface and outlet (cf. Fig. 5). It is noted that for injected solutions of lower density, the dye reaches the drop surface first in the top edge via the reversed flow. The effects of solution density on changes in DIC and DOC for dt = 0.33 s and dV = 0.067 mm^3/pulse are shown in Fig. 15. While a significant drop interfacial exchange (about 90%) is achieved within 100 s and simultaneously high DOC values, the drop surface exchange for the injected solution of lower density is only 50% with simultaneously high values of DOC. This means that a much longer exchange time is needed for a proper interfacial exchange. The results obtained from Eqs. (1) and (2) for perfect mixing are also presented in this figure. As for this simple assumption no density effects are considered, a significant error in the prediction for DIC appears. The observed oscillations in the DOC curves (e.g. Figs. 14 and 15) can be related to an unsteady pulse-like input solution which can affect the DOC values directly. The other reason can be a computational instability due to the mentioned pulse-like flow.

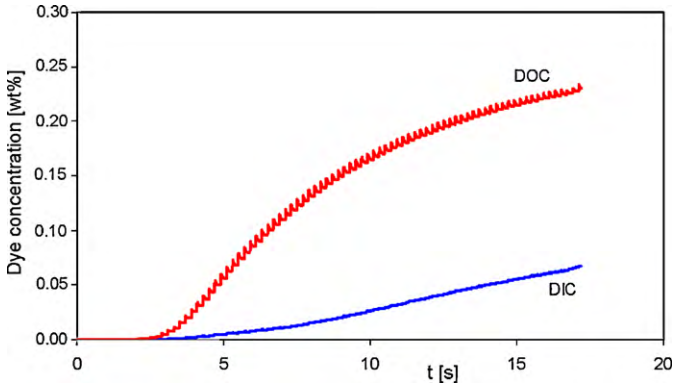

Fig. 14. Drop interface concentration (DIC) lower than drop outlet concentration (DOC) for low density dye solution (+1.5% ethanol), dt = 0.2 s and dV = 0.1 mm^3/pulse.

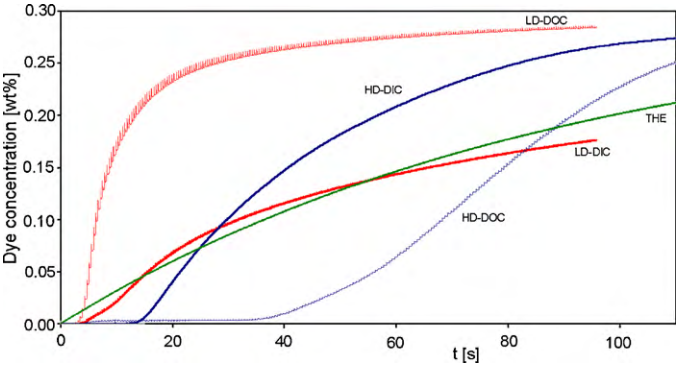

Fig. 15. Effects of solution density on CFD results for DIC and DOC evolution for dt = 0.33 s, and dV = 0.067 mm^3/pulse. LD = low density, HD = high density solution, and THE = theoretical modeling assuming perfect mixing.

6. Conclusion

Despite the small size of pendant drops used in drop profile tensiometry, the coaxial double capillary allows an efficient drop bulk exchange. Choosing the right experimental conditions for an efficient drop exchange disturbances and drop shaking can be avoided. Flow visualization using dye solutions for exchange and CFD simulation demonstrate details for the optimization of this interesting experimental tool and improve the understanding of the effects of basic parameters, which can be summarized as follows:

- The liquid exchange process can be visualized by injection of dye solutions and are comparable with CFD simulation, until the moment Marangoni convection sets in. The CFD results for the drop interfacial concentration (DIC) and drop outlet concentration (DOC) are in good agreement with observed experimental images and measured surface tension data before the onset of Marangoni convection. Although Marangoni convection enhances mass transfer at the drop surface and in the bulk significantly, it should be better avoided to allow for a quantitative evaluation of adsorption or desorption processes at the drop surface.
- Density differences between drop and injected liquids influence the structure of the circulating flow significantly even for small $\Delta\rho$. For the injection of lower density solutions, a quick reverse flow is the major barrier for a perfect drop exchange. To avoid to drop perturbation effects and instabilities, at sufficiently low injection rates dV the drop exchange can be improved by a larger immersed depth of the inner capillary into the drop.
- The consideration of the trends and distance of the DIC and DOC curves obtained by CFD simulation provides a useful tool for understanding the exchange process mechanism and finding optimum process parameters.
- Simplified theoretical models assuming a perfect mixing show significant errors in the prediction of DIC and DOC, while the presented combination of dye injection and CFD simulation provide a sufficiently accurate tool.

Acknowledgements

The work was financially supported by a project of the German Space Agency (DLR 50WM0941) and the DFG (Mi418/16-1). The authors are also very grateful for the important support by K. Javadi in the performance of the CFD simulations.

References

[1] Y. Rotenberg, L. Boruvka, A.W. Neumann, J.Colloid Interface Sci. 93 (1983) 169–183.
[2] P. Cheng, A.W. Neumann, Colloid Surf. 62 (1992) 297–305.
[3] G. Loglio, P. Pandolfini, R. Miller, A.V. Makievski, F. Ravera, M. Ferrari, L. Liggieri, Drop and bubble shape analysis as tool for dilational rheology studies of interfacial layers, in: D. Möbius, R. Miller (Eds.), Novel Methods to Study Interfacial Layers, vol. 11, Elsevier, 2001.
[4] H.A. Wege, J.A. Holgado-Terriza, A.W. Neumann, M.A. Cabrerizo-Vilchez, Colloid Surf. A 156 (1999) 509–517.
[5] T.F. Svitova, M.J. Wetherbee, C.J. Radke, J. Colloid Interface Sci. 261 (2003) 170–179.
[6] V.B. Fainerman, M.E. Leser, M. Michel, E.H. Lucassen-Reynders, R. Miller, J. Phys. Chem. B 109 (2005) 9672–9677.
[7] J.K. Ferri, N. Gorevski, Cs. Kotsmar, M.E. Leser, R. Miller, Colloid Surf. A 319 (2008) 13–20.
[8] J.K. Ferri, W.-F. Dong, R. Miller, J. Phys. Chem. B 109 (2005) 14764–14768.
[9] V.B. Fainerman, A.V. Makievski, J. Krägel, A. Javadi, R. Miller, J. Colloid Interface Sci. 308 (2007) 249–253.
[10] J.K. Ferri, Cs. Kotsmar and R. Miller, Adv. Colloid Interface Sci., in press.
[11] H.A. Wege, J.A. Holgado-Terriza, M.A. Cabrerizo-Vilchez, J. Colloid Interface Sci. 249 (2002) 263–273.
[12] N.M. Kovalchuk, D. Vollhardt, Adv. Colloid Interface Sci. 120 (2006) 1–31.